Additive Manufacturing 48 (2021) 102408

Contents lists available at ScienceDirect

Additive Manufacturing

journal homepage: www.elsevier.com/locate/addma

Research Paper

Water-soluble sacrificial 3D printed molds for fast prototyping in ceramic injection molding

René Wick-Joliat, Maurice Tschamper, Roman Kontic, Dirk Penner *

Institute of Materials and Process Engineering, ZHAW Zürcher Hochschule für Angewandte Wissenschaften, Technikumstrasse 9, 8401 Winterthur, Switzerland

ARTICLE INFO

Keywords:
Freeform injection molding
Ceramic injection molding
Two-component injection molding
3D printed injection mold
Sacrificial injection mold
$MoSi_2$ heating element

ABSTRACT

Fabrication of steel molds is a major expense (time and cost) in ceramic injection molding research and development. 3D printed resin molds for fast prototyping are therefore highly attractive and have gained increasing attention. This paper reports strategies to use sacrificial molds 3D printed by fused deposition modeling (FDM) from PVA or digital light processing (DLP) from water soluble resin. Usage of sacrificial molds allows injection molding of complex geometries, which are not accessible for simple two-part molds. Ceramic heating elements in diverse geometries were injection molded using a composite feedstock containing $MoSi_2$, Al_2O_3 and feldspar. More parts with various geometries were produced from Al_2O_3 feedstock. A comparison revealed that DLP printed molds are better suited for parts with very small structural features due to the higher resolution of the DLP process as compared to FDM. Finally, ceramic heaters were fabricated using two-component ceramic injection molding and successfully tested.

1. Introduction

Ceramic injection molding (CIM) is routinely used to fabricate ceramic parts of all shapes, sizes and ceramic materials [1,2]. During CIM, a ceramic powder plastified by a thermoplastic binder is injected at high pressure into a closed mold. The feedstock cools down and solidifies to give the green body, which is then debound (removal of the binder by solvent and/or thermally) and sintered. Due to its high throughput, CIM is very economical for parts fabricated in large quantities. However, mold making is time consuming and expensive and once the mold is fabricated, changes in the geometry of the molded parts can hardly be incorporated [3]. An example of a simple steel mold is shown in Fig. 1A. 3D printed molds provide a cheap and fast alternative to classical steel molds for prototyping purposes or low volume production [4–8]. The 3D printed mold is typically inserted into a steel adapter piece with cavities on both sides (Fig. 1B). The 3D printing method of choice is usually stereolithography (SLA) or direct light processing (DLP) due to their higher dimensional accuracy and smooth surface of the printed molds in comparison to fused deposition modeling (FDM). 3D printed molds are mostly limited to simple straight-pull molds with two sides as shown in Fig. 1C. Freeform injection molding (FIM) is a novel method to overcome this limitation [9–11]. In FIM, the mold is 3D printed from a soluble resin and is dissolved after injection molding. The usage of sacrificial molds opens up new possibilities for more complex geometry since design restrictions regarding undercuts do not apply. One example of a sacrificial mold is shown in Fig. 1D.

The advantages of 3D printed sacrificial molds over classical hardened steel molds are summarized in Table 1. Most importantly, fabrication of 3D printed sacrificial molds is considerably faster and less expensive. A point that should not be underestimated is that prototyping using 3D printed sacrificial molds is feasible for any small company, laboratory or start-up, since the requirements for heavy machinery and highly specialized operators are lower. It should be mentioned that a detailed cost analysis would be dependent on many factors including cost of the material, cost of the 3D printers, cost of other equipment, cost of energy, cost of labor etc. Every single one of those factors has a huge cost range depending on the geometry, size, quantity and material of the desired part. The same is true for machined molds. In summary, a detailed cost analysis is beyond the scope of this study and just a broad cost range based on our experience is given in Table 1.

In this paper, FIM and CIM are combined to produce high quality ceramic parts with complex geometries that could not be injection molded with any other method. For the first time, sacrificial molds are printed from polyvinylalcohol (PVA) in an FDM printer. FDM printed PVA molds withstand the harsh conditions during injection molding (high pressure and temperature) and yield high quality parts of even

* Corresponding author.
E-mail address: dirk.penner@zhaw.ch (D. Penner).

https://doi.org/10.1016/j.addma.2021.102408
Received 16 July 2021; Received in revised form 28 September 2021; Accepted 12 October 2021
Available online 16 October 2021

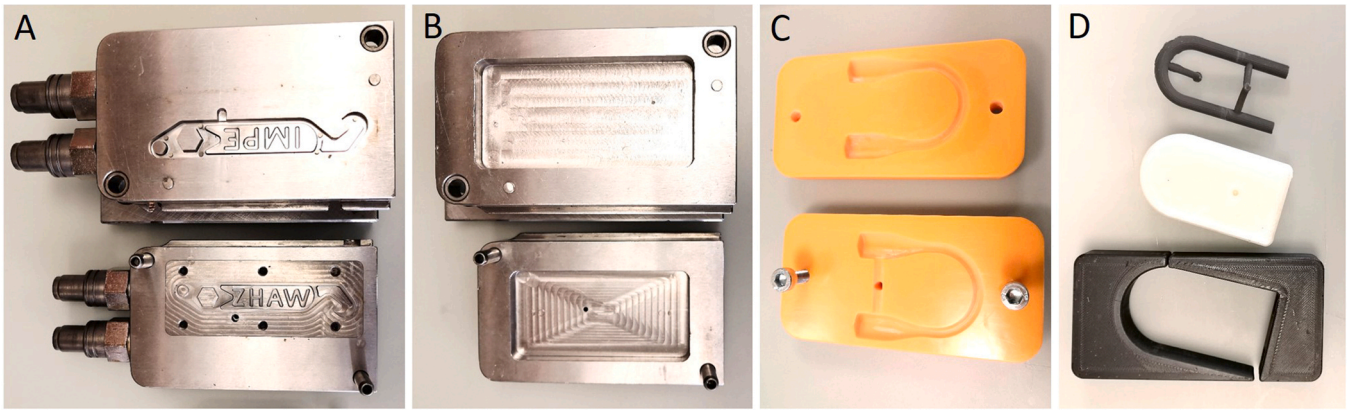

Fig. 1. Steel mold (A). Steel adapter with cavities on both sides that can hold the 3D printed mold (B). Resin mold 3D printed by DLP (C). Injection molded part after dissolving the sacrificial mold (D, top), the sacrificial mold itself (D, center) and an adapter piece to fit the sacrificial mold into the steel adapter (D, bottom).

Table 1
Comparison of injection molding process using classical steel molds versus 3D printed sacrificial molds.

Method	Steel mold	3D printed sacrificial mold
Application	Industrial production	Fast prototyping
Number of pieces	> 10′000	1–20
Time for mold making	Weeks to months	Few days
Cost of the mold	10′000–100′000 $ (strongly depending on complexity)	< 10 $
Equipment	Specialized workshop	3D printer (FDM or SLA or DLP)
Skill required	Specialized moldmaker	Basics in CAD and 3D printing

complex geometries. Parts were molded from commercial Al_2O_3 feedstock as well as from a composite feedstock developed in our lab containing $MoSi_2$ particles [12]. $MoSi_2$ is an electrically conductive intermetallic material with thermal stability up to 1800 °C and is therefore common in high temperature applications [13,14]. $MoSi_2$ containing samples were tested in glowing experiments to show that they can be used as resistive heating elements.

For comparison to the FDM printed PVA molds, sacrificial molds were also printed from resin by direct light processing (DLP). A resin recipe from literature [15] was adapted to yield water soluble molds with higher resolution than PVA molds printed by FDM. Higher resolution allows the injection molding of parts with finer details, as demonstrated on a screw thread, and smoother surface.

Two component injection molding (2 C-IM) is widely known in thermoplastics industry [16–18]. The method is relatively straightforward for thermoplastics, but poses additional problems in CIM, mainly since the shrinkage behavior of the two materials during sintering has to be matched carefully. Examples of 2 C-CIM are therefore scarce [19–26]. In the last part of the present study, 2 C-CIM using sacrificial 3D printed molds is demonstrated for the first time. The two target parts were a $MoSi_2$ heating element with zones of different electrical conductivity as well as a nonconductive crucible with integrated conductive heating coil.

2. Materials and methods

All CAD was done in Fusion 360 software from Autodesk.

PVA molds were printed using an Ultimaker 3 FDM printer and PVA filament supplied by Ultimaker. Layer height was set to 0.1 mm and wall thickness to 6 lines. A triangular infill with 50% infill density was used. Otherwise, the standard settings for PVA as recommended by Ultimaker were used.

Sacrificial molds were also printed on an Asiga Max X DLP printer using a resin formulation reported by Liska et al.[15] N, N-Dimethylacrylamide (20 g, 99%, Aldrich), Methacrylic acid (20 g, 99%, abcr) and Methacrylic anhydride (3.5 g, 94%, Sigma-Aldrich) were added to a beaker, Polyvinylpyrrolidone (6.5 g, MW 10′000, Sigma-Aldrich) was added portionwise and the solution was stirred and ultrasonicated until the PVP dissolved completely. Phenylbis(2,4,6-trimethylbenzoyl)phosphine oxide (1 g, 96%, abcr) and solvent yellow 93 (0.015 g) were added and stirred until a clear solution was obtained. The solution was filtered before usage in DLP. The following

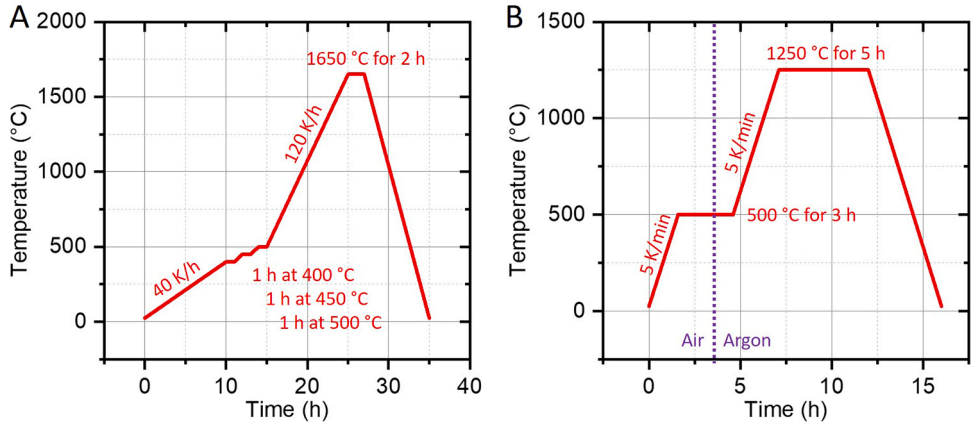

Fig. 2. Thermal debinding and sintering conditions for Al_2O_3 parts (A) and $MoSi_2$ parts (B).

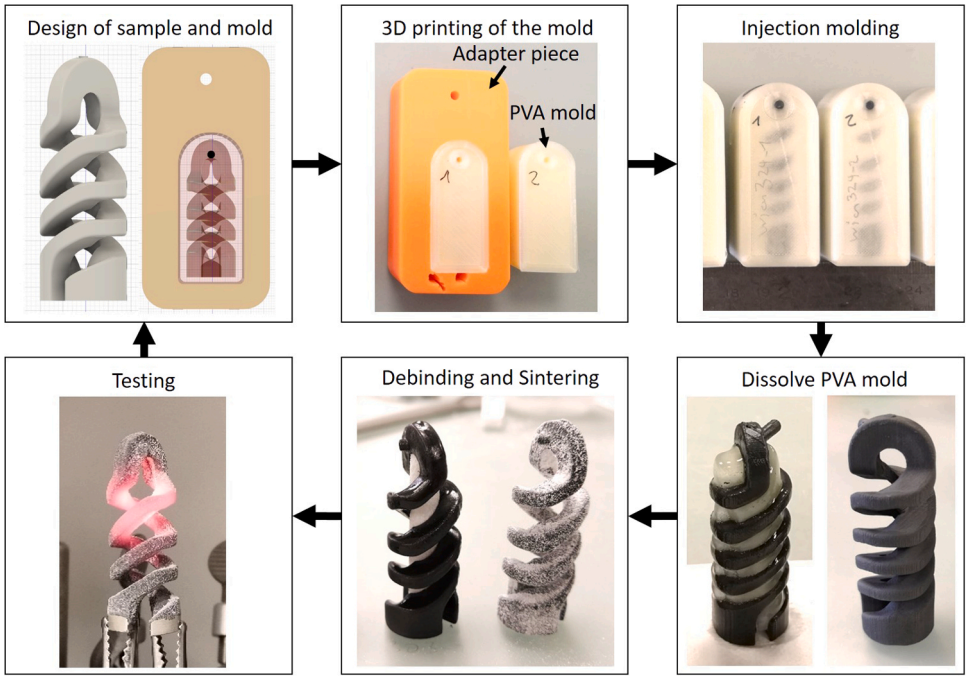

Fig. 3. Overview of the prototyping workflow with sacrificial injection molds for CIM. Details explained in the main text.

printing parameters were used: Layer thickness: 25 μm; Exposure time: 10 s; Light intensity: 4 mW/cm^2.

Adapter pieces for mounting the sacrificial molds to the injection molding machine were printed on a SL1 DLP printer from Prusa with either tough orange resin from Prusa or Standard Blend Red from FunToDo or by FDM from black ABS on an Ultimaker 3. Both resins were printed using the default settings for tough orange resin. ABS was printed using the default settings provided by Ultimaker with 0.1 mm layer height, an infill density of 50% and 6 lines wall thickness.

CIM feedstocks were either bought or prepared in-house. Al_2O_3 feedstock was supplied by Krahn Ceramics. $MoSi_2$ feedstocks were prepared as previously reported [12]: $MoSi_2$ (H.C.Starck, Grade A), Al_2O_3 (Almatis, CT19FG) and feldspar (Sibelco) were homogenized together with the commercial binder system Embemould K83 (92 wt%, Krahn Ceramics) and LDPE (8 wt%, LD 655, Exxon mobile) using a twin-screw extruder (Thermo Fischer, Process11 Extruder). After extrusion, the feedstock was cooled down to 50–70 °C and blended in a Nutri Bullet 600 blender. All feedstocks underwent 5–7 extrusion and blending cycles before being used for injection molding. Powder loading was 56 vol % with different $MoSi_2/Al_2O_3$ ratios depending on the desired conductivity of the final part.

Injection molding was performed on a BOY XS machine. All feedstocks were injected at 150 °C with pressures of 40–80 bar, depending on the feedstock and mold geometry.

PVA molds were dissolved in a water bath at 40 °C. The water was exchanged as soon as the PVA was fully dissolved and the green parts were immersed at 40 °C for additional 4 – 6 days for solvent debinding.

Sacrificial resin molds were dissolved in 0.1 M NaOH at 50 °C. After complete dissolution of the resin, the green parts were rinsed with water and immersed in a water bath at 40 °C for additional 4 – 6 days for solvent debinding.

After the solvent debinding step, all samples were dried in an oven at 40 °C for at least 24 h.

Thermal debinding and sintering was performed according to the heating profiles in Fig. 2. For Al_2O_3 samples, thermal debinding was done stepwise with holding periods at 400, 450 and 500 °C and sintering at 1650 °C. For $MoSi_2$ containing parts, thermal debinding was performed in air atmosphere at 500 °C before switching to argon atmosphere while keeping the temperature for one more hour at 500 °C. For sintering, the oven was heated under argon to 1250 °C and kept at this temperature for 5 h. Some $MoSi_2$ parts were sintered in an Al_2O_3 powder bed to avoid structural deformations during sintering.

For the glow tests, the surface of the contact arms of the sintered samples was ground using a Dremel minidrill tool and subsequently coated with colloidal Silver paste. Current and voltage were controlled by a TDK-Lambda Gen300–11 power source.

SEM imaging was conducted on a Phenom XL Desktop SEM (Thermo Fischer Scientific).

3. Results and discussion

In the design of a sample for FIM, many of the design rules for classical injection molding parts do not apply. Most importantly, undercuts are allowed. This drastically increases design freedom and complex structures such as spirals are moldable without special consideration to avoid undercuts. The sacrificial mold is then designed by constructing a cube or cylinder, which is at least 1 mm bigger than the ceramic sample in all directions, and subtracting the ceramic part from the mold. Gates and vents are added according to the specifications of the injection molding machine used. For the example shown in Fig. 3a double helix with three turnings was designed. The wall thickness in this example is 4 mm. The part was subtracted from a rectangular block with rounded edges and the gate was placed at the top arch of the helix. This block was printed on an Ultimaker 3 from PVA filament. For most PVA molds, infill densities of 100% were used to obtain maximal strength. However, lower infill densities of 50% were also successfully tested, but the wall thickness was set to at least 1 mm. An adapter piece was designed and printed from UV-curable resin on a Prusa SL1.

The parts were injection molded on a BOY XS machine using commercial Al_2O_3 feedstock or $MoSi_2$/Feldspar/Al_2O_3 composite feedstock developed in our laboratory [12]. Two drawbacks of the method presented herein are the limited injection pressure and temperature. The double helix shown in Fig. 3 was successfully molded using injection pressures of 50–90 bar. With lower pressures, the PVA mold is not filled completely, while higher pressures lead to cracking of the PVA mold. It was found that the injection temperature should be below 150 °C, since

Fig. 4. Examples of heating elements designed for injection molding using 3D printed PVA molds. CAD drawings of the target parts together with the respective PVA molds (A). Green bodies after injection molding and dissolving the PVA molds (B). Sintered spiral part in glowing test at 460 W power input (C).

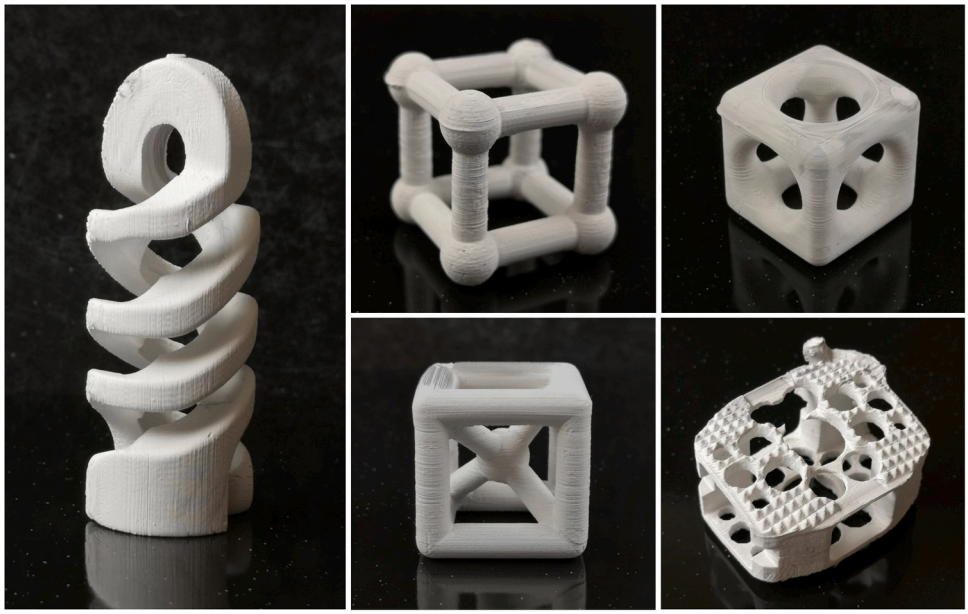

Fig. 5. Collection of green bodies molded using PVA molds and Al_2O_3 feedstock. All geometries have undercuts that could not be molded with a two-part steel mold.

the PVA mold already softens at this temperature. This factor reduces the choice of binder systems for preparation of the feedstock. Nevertheless, all feedstocks based on LDPE, EVA, PEG, and other low melting temperature polymers are still feasible. However, the temperature limitation does not apply to sacrificial molds printed from water soluble resin. Additionally, the feedstock must not take damage in contact with water (swelling etc.), since after injection molding, PVA molds were immersed in a water bath to dissolve the PVA. This process takes from 12 h up to two days, depending on the size and geometry as well as the infill density used to print the PVA mold and on how frequently the water bath is exchanged. Ideally, the water bath also serves to pre-debind the molded parts if the feedstock contains a water-soluble auxiliary binder.

The remaining steps are identical to classical CIM: green body processing, thermal debinding, sintering, and finally testing of the finished part. The advantage of the method presented herein lies in the fact that this "designing – manufacturing – testing" cycle can be repeated very cost and time efficiently.

Fig. 4 shows a collection of green bodies injection molded in PVA molds with a $MoSi_2/Al_2O_3$/Feldspar feedstock. Those samples were thermally debound in air and sintered in argon atmosphere. Due to the $MoSi_2$ content, the samples are conductive after sintering and are used as heating elements (Fig. 4C). While some of the parts shown in Fig. 4 could be molded with a simple straight-pull steel mold, the helix and the spiral would require at least an additional side-action core, making the steel mold much more complicated and expensive. For 3D printed PVA molds,

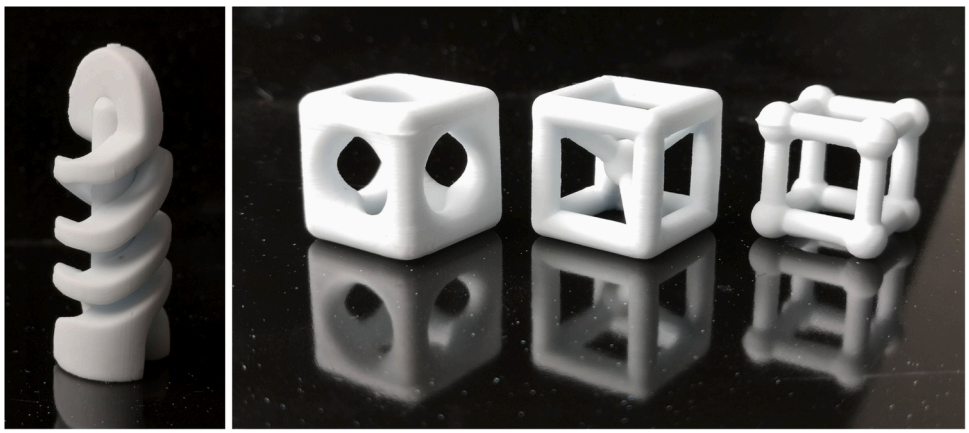

Fig. 6. Sintered Al_2O_3 samples. Height of the helix: 42 mm, side length of the cubes: 20 mm.

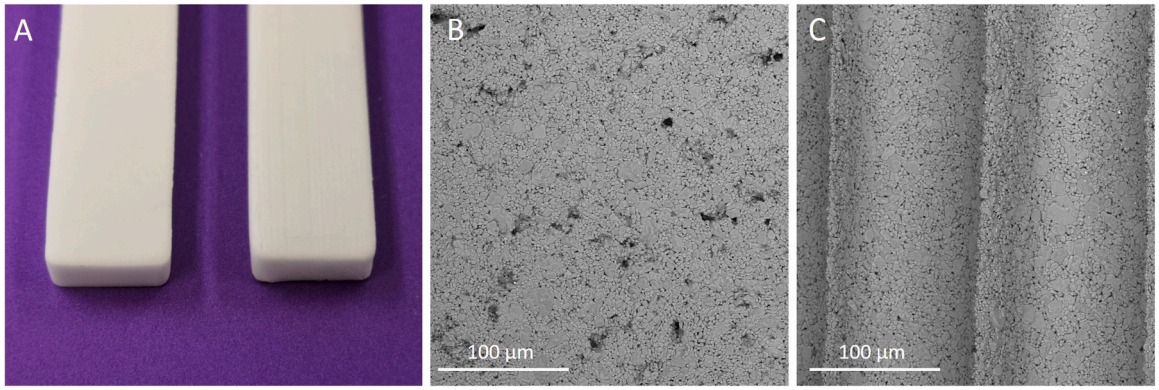

Fig. 7. Photograph of injection molded and sintered parts. Left: steel mold. Right: 3D printed PVA mold (A). SEM image of the surface of the rod fabricated with the steel mold (B). SEM image of the surface of the sample produces with a PVA mold showing the typical line structure arising from a FDM 3D printer (C).

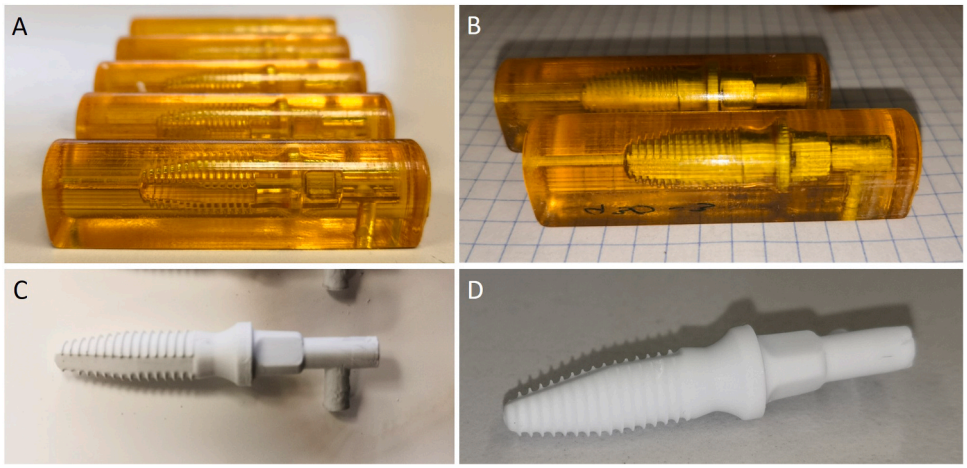

Fig. 8. Production of dental implant prototypes: Sacrificial resin molds printed by DLP (A). Filled mold after injection molding with a commercial Al_2O_3 feedstock (B). Green part after dissolving the sacrificial mold in 0.1 M NaOH (C). Sintered part (D).

undercuts and complex geometries do not increase the cost and time required to fabricate the mold.

More examples of samples with complex geometries are displayed in Fig. 5 (green bodies) and Fig. 6 (sintered samples). Those parts were molded using an Al_2O_3 feedstock. The spinal disk prosthesis (Fig. 5, bottom right) features some bridges as thin as 0.8 mm as well as a pyramidal surface with pyramids of 1.5 mm side length, proving that even delicate structures can be fabricated with PVA molds.

The surface morphology of rod-shaped samples injection molded with a steel mold and a 3D printed PVA mold were compared by SEM (Fig. 7). The fine lines on the PVA mold samples are visible by eye and SEM and originate from the filament 3D printing of the PVA mold. The distance between the lines therefore corresponds to the layer height used for 3D printing which was 0.1 mm in the case of the sample in Fig. 7. If those lines are undesired, the green bodies could be sanded or polished before sintering. No differences are visible between steel mold and PVA

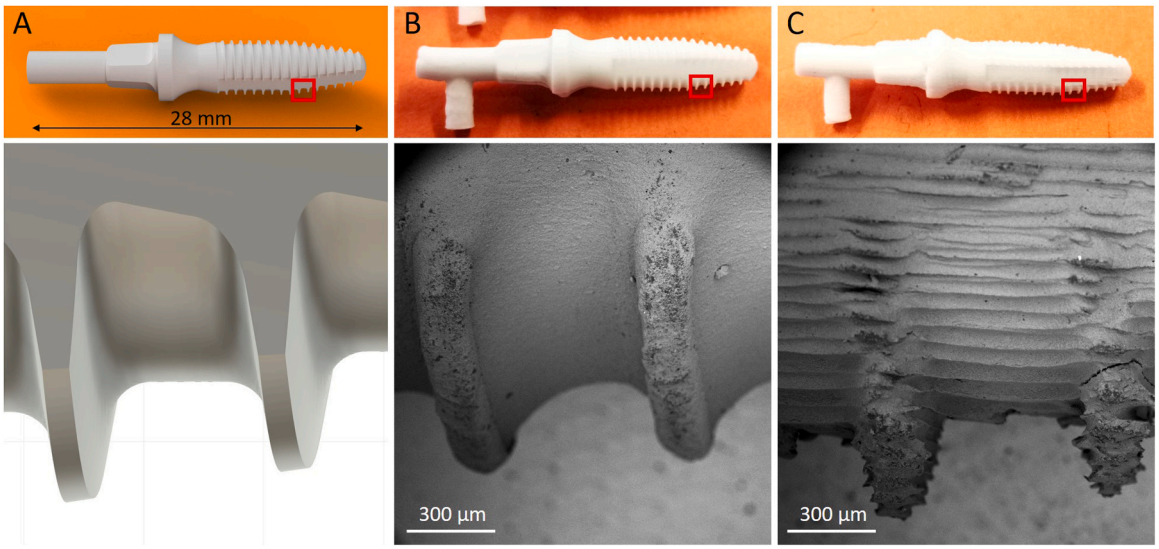

Fig. 9. Comparison of a threaded part as CAD file (A) and sintered parts fabricated using an DLP resin mold (B) as well as FDM printed PVA mold (C).

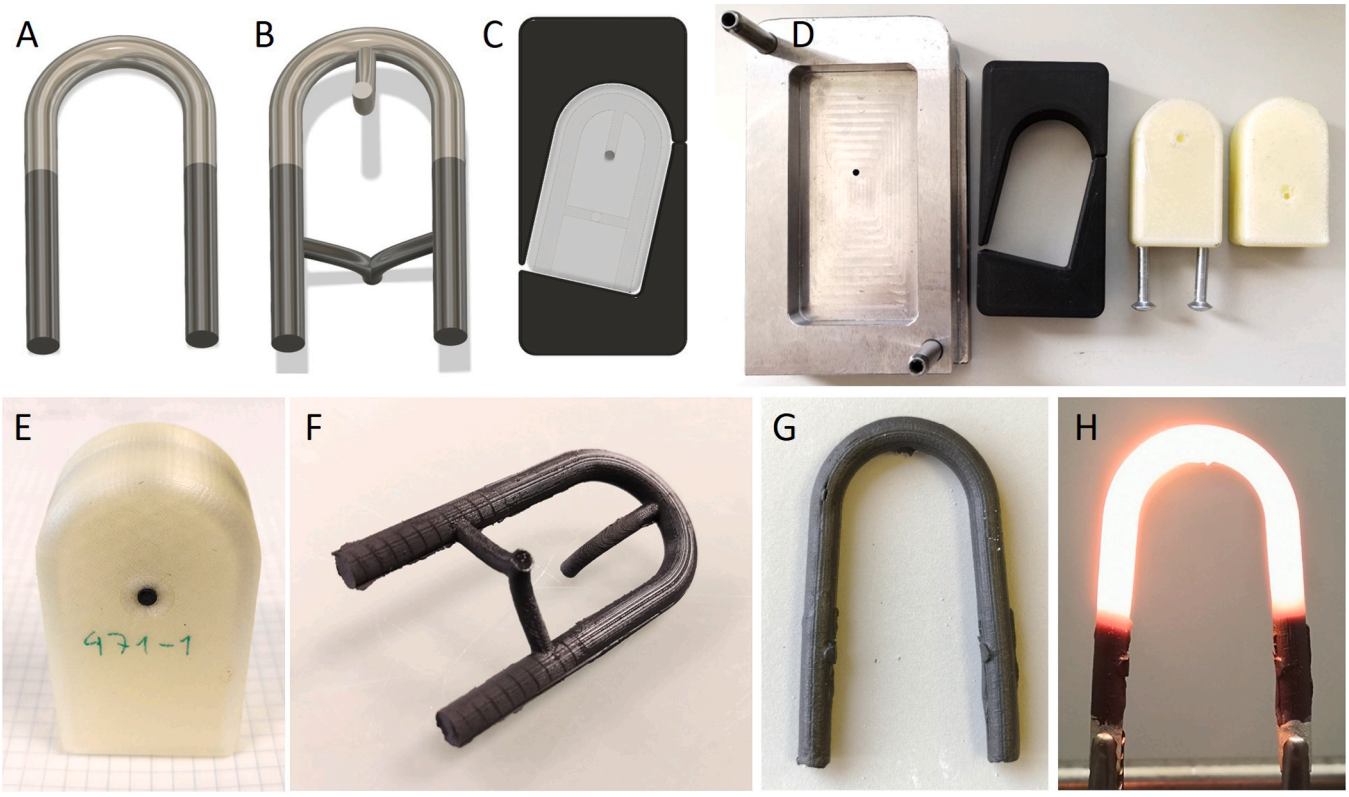

Fig. 10. Different stages of 2 C-CIM with a PVA mold. CAD drawings of the target part with low conductivity in the arch and higher conductivity in the arms (A). Gates added for frontside and backside injection of the two feedstocks (B). PVA negative form and ABS adapter pieces (C). Steel tool and FDM printed ABS adapter and PVA mold. Two screws are used during injection molding of the arch and subsequently removed for injection of the arms (D). PVA mold after injection of both materials from two sides (E). Green body after dissolution of the PVA in water (F). Final part after sintering (G). Glow test showing glowing only in the arch since resistance is higher than in the contact arms (H).

samples in the bulk of the material.

Sacrificial molds for injection molding can also be 3D printed by stereolithography (SLA) or direct light processing (DLP) using a water-soluble resin. For this purpose, a resin recipe reported by Liska et al. was adapted [15]. Dimethylacrylamide and methacrylic acid were used as the monomers to ensure fast curing and solubility in water. Polyvinylpyrrolidone was added as a filler and together with the crosslinker methacrylic acid anhydride increased the resolution. The dye Solvent Yellow 93 was found to improve curing times and overall print quality.

The sacrificial molds shown in Fig. 8 were rinsed with acetone after printing to wash away any excess of non-cured resin inside the mold. Injection molding with resin molds is identical to the process described above with PVA molds. The sacrificial mold was then dissolved in basic aqueous solution (0.1 M NaOH) at 50 °C. This process completely dissolved the mold in less than 12 h and the green parts were immersed in a water bath for pre-debinding for a few days, according to the auxiliary

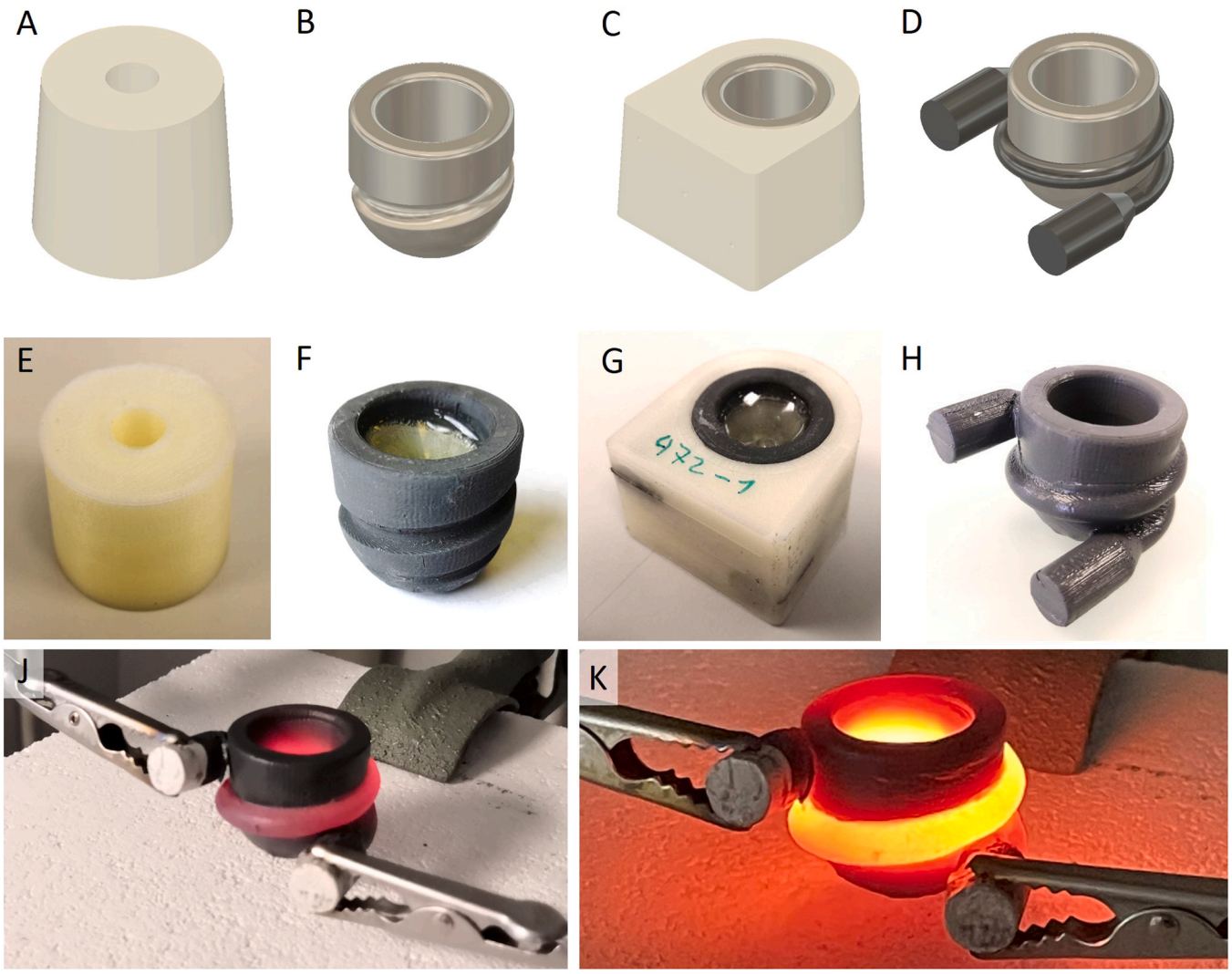

Fig. 11. Different fabrication stages of 2 C-CIM with two PVA molds. CAD drawings (A-D) and photographs (E-K). The first PVA mold (A, E) is used to injection mold the crucible (B, F), which is then pressed into the second PVA mold (C, G) into which the heating coil consisting of conductive $MoSi_2$ ceramic composite is injected. In this stage, PVA inside the crucible is not fully dissolved and gives additional stability during the injection molding of the heating coil. The 2 C green body is obtained by dissolving the second PVA mold in water (H). Glow tests of the sintered part at 110 W (J) and 210 W (K).

binder used in the feedstock. The Al_2O_3 dental implant prototypes shown in Fig. 8D underwent debinding and sintering at 500/1650 °C to give the final parts.

In general, SLA and DLP both have a higher resolution than FDM [27] since the size of the laser used in SLA (approx. 0.1 mm) or the pixel size in DLP (0.05–0.1 mm) is smaller than the nozzle used in FDM (typically 0.4 mm). For parts with filigree details such as a screw thread (Fig. 8, Fig. 9), printing a mold by SLA or DLP is preferential. The resolution difference is clearly visible in Fig. 9, where the CAD image is compared to sintered parts molded from DLP resin molds and FDM PVA molds. In this example, the layer height and line width used for FDM are too close to the dimensions of the screw thread, whereas DLP can provide the required high resolution. It should be noted that the printing direction plays a crucial role in FDM and to a lesser extent in DLP. Therefore, the quality of the screw thread in Fig. 9C could be improved by printing the mold horizontally instead of vertically. Nevertheless, the resolution would still be surpassed by DLP or SLA.

Two component ceramic injection molding (2 C-CIM) is also possible using FDM printed PVA molds. A U-shaped heating element was chosen as a proof of concept part. Classically, those parts consist of a thin arch and much thicker contact arms, so that only the arch glows due to the higher resistivity [28]. A different approach is the usage of two different materials with lower conductivity for the arch and higher conductivity for the contact arms [26]. For this purpose, $MoSi_2/Al_2O_3$/feldspar composites with $MoSi_2$ content of 15 vol% and 18 vol% were chosen for the arch and contacts, respectively. Firstly, PVA mold and ABS adapter pieces were designed by CAD (Fig. 10A-C). The gates for the two materials were added in such a way that the materials could be injected from two sides of the PVA mold by turning the PVA mold around after injecting the first material. For the injection of the arch two screws were used as place holders for the contact arms. After the first injection, the screws were removed, the PVA mold was turned around and the second feedstock was injected from the backside (Fig. 10D-E). PVA was then dissolved in water at 40 °C and the parts were simultaneously pre-debound. Next, the green bodies were thermally debound and sintered (Fig. 10F-G). Finally, the feasibility of the method was proven by glow tests showing that only the arch of the part glows while the more conductive contact arms remain much colder (Fig. 10H).

An additional approach to 2 C-CIM was employed to fabricate a ceramic crucible with integrated heating coil (Fig. 11). For this purpose, a non-conductive crucible was molded using a PVA mold. After dissolving the PVA mold, the green body was pressed into the PVA mold for the heating coil. Two similar feedstocks were used for the crucible and heating coil to assure compatible sintering behavior of the components

and avoid mechanical stress and improper sintering in the final parts. For the crucible, a $MoSi_2$/Feldspar/Al_2O_3 composite with a low $MoSi_2$ content of 10 vol% yielded an insulating crucible. For the heating coil, the same composite with 18 vol% $MoSi_2$ content gave the desired conductivity. Glow tests then showed that the sintered 2 C crucible worked as intended (Fig. 11J-K).

4. Conclusion

Freeform injection molding (FIM) with sacrificial molds is a promising tool to speed up prototyping. In this study, FIM is extended to ceramic feedstocks to produce a variety of parts with demanding geometries such as spirals, cages and helices from Al_2O_3 feedstock as well as $MoSi_2$ containing composite. The injection molds were FDM printed from PVA. This fast and simple method is limited when it comes to very fine structural details. Therefore, a screw thread was fabricated using FDM printed PVA molds as well as DLP printed sacrificial molds. This comparison showed that DLP printed molds are indeed preferable when very high resolution is required. Lastly, the potential of sacrificial molds for 2 C-CIM was demonstrated by fabricating a $MoSi_2$ heating element with higher conductivity in the contacting arms as well as a ceramic crucible with integrated heating coil. Both samples were successfully operated in glowing tests.

Funding

Some of the results of this work were produced within the framework of Swiss Innovation Agency – Innosuisse funded projects 29990.1 IP-ENG and 30021.1 IP-ENG.

CRediT authorship contribution statement

René Wick-Joliat: Conceptualization, Investigation, Visualization, Writing – original draft. **Maurice Tschamper**: Investigation. **Roman Kontic**: Conceptualization, Investigation. **Dirk Penner**; Writing – review & editing, Supervision.

Declaration of Competing Interest

The authors declare that they have no known competing financial interests or personal relationships that could have appeared to influence the work reported in this paper.

Acknowledgment

The authors would like to thank Leister Technologies AG and Metoxit AG for their cooperation and support as well as Sijia Liu for taking photos shown in Fig. 11.

References

[1] B.C. Mutsuddy, R.G. Ford, Ceramic Injection Molding, Chapman & Hall, London, 1994.
[2] R.M. German, A. Bose, Injection Molding of Metals and Ceramics, Metal Powder Industries Federation, Princeton, N.J., 1997.
[3] R. Gadow, F. Kern, Advanced manufacturing of hard ceramics, in: Compr. Hard Mater., Elsevier, 2014, pp. 207–230, https://doi.org/10.1016/B978-0-08-096527-7.00025-8.
[4] N. Hopkinson, P. Dickens, Predicting stereolithography injection mould tool behaviour using models to predict ejection force and tool strength, Int. J. Prod. Res. 38 (2000) 3747–3757, https://doi.org/10.1080/00207540050175987.
[5] P.K.D.V. Yarlagadda, L.K. Wee, Design, development and evaluation of 3D mold inserts using a rapid prototyping technique and powder-sintering process, Int. J. Prod. Res. 44 (2006) 919–938, https://doi.org/10.1080/00207540500140880.
[6] G.A. Mendible, J.A. Rulander, S.P. Johnston, Comparative study of rapid and conventional tooling for plastics injection molding, Rapid Prototyp. J. 23 (2017) 344–352, https://doi.org/10.1108/RPJ-01-2016-0013.
[7] A. Bagalkot, D. Pons, D. Symons, D. Clucas, Analysis of raised feature failures on 3D printed injection moulds, Polym. (Basel) 13 (2021) 1541, https://doi.org/10.3390/polym13101541.
[8] S. Krizsma, N.K. Kovács, J.G. Kovács, A. Suplicz, In-situ monitoring of deformation in rapid prototyped injection molds, Addit. Manuf. 42 (2021), 102001, https://doi.org/10.1016/j.addma.2021.102001.
[9] A. Basso, M. Mendez Ribo, A. Halina Danielak, B. Yang, P. Kjeldsteen, P. Valler, D. Bue Pedersen, Y. Zhang, 3d Printed Mold for Powder Injection Molding Process, Proc. Jt. Spec. Interes. Gr. Meet. between Euspen ASPE Adv. Precis. Addit. Manuf., 2019: 71–74. ⟨www.euspen.eu⟩.
[10] E. Sharifi, A. Chaudhuri, B.V. Wæhrens, L.G. Staal, S.D. Farahani, Part selection for freeform injection molding: framework for development of a unique methodology, in: B. Lalic, V. Majstorovic, U. Marjanovic, G. von Cieminski, D. Romero (Eds.), Adv. Prod. Manag. Syst. Towar. Smart Digit. Manuf., Springer International Publishing, Cham, 2020, pp. 723–730.
[11] E. Sharifi, A. Chaudhuri, B.V. Waehrens, L.G. Staal, S. Davoudabadi Farahani, Assessing the suitability of freeform injection molding for low volume injection molded parts: a design science approach, Sustainability 13 (2021) 1313, https://doi.org/10.3390/su13031313.
[12] R. Wick-Joliat, S. Mauchle, R. Kontic, S. Ehrat, T. Hocker, D. Penner, $MoSi_2$/Al_2O_3/Feldspar Composites for Injection-Molded Ceramic Heating Elements, Adv. Eng. Mater. 232100517 (2021), https://doi.org/10.1002/adem.202100517.
[13] Y.L. Jeng, E.J. Lavernia, Processing of molybdenum disilicide, J. Mater. Sci. 29 (1994) 2557–2571, https://doi.org/10.1007/BF00356804.
[14] Z. Yao, J. Stiglich, T.S. Sudarshan, Molybdenum silicide based materials and their properties, J. Mater. Eng. Perform. 8 (1999) 291–304, https://doi.org/10.1361/105994999770346837.
[15] R. Liska, F. Schwager, C. Maier, R. Cano-Vives, J. Stampfl, Water-soluble photopolymers for rapid prototyping of cellular materials, J. Appl. Polym. Sci. 97 (2005) 2286–2298, https://doi.org/10.1002/app.22025.
[16] W. Zoetelief, Multi-component injection moulding, Tech. Univ. Eindh. (1995), https://doi.org/10.6100/IR435035.
[17] A.G. Banerjee, X. Li, G. Fowler, S.K. Gupta, Incorporating manufacturability considerations during design of injection molded multi-material objects, Res. Eng. Des. 17 (2007) 207–231, https://doi.org/10.1007/s00163-007-0027-9.
[18] V. Goodship, J.C. Love, Multi-Material Injection Moulding, Smithers Rapra Technology, 2002.
[19] A. Ruh, K. Klimscha, V. Piotter, K. Plewa, H.-J. Ritzhaupt-Kleissl, J. Fleischer, The development of two-component micro powder injection moulding and sinter joining, Microsyst. Technol. 17 (2011) 1547–1556, https://doi.org/10.1007/s00542-011-1326-7.
[20] A. Basir, A.B. Sulong, N.H. Jamadon, N. Muhamad, Bi-material micro-part of stainless steel and zirconia by two-component micro-powder injection molding: rheological properties and solvent debinding behavior, Met. (Basel). 10 (2020) 595, https://doi.org/10.3390/met10050595.
[21] A. Ruh, V. Piotter, K. Plewa, H.-J. Ritzhaupt-Kleissl, J. Hausselt, Development of two-component micropowder injection molding (2C-MicroPIM)-process development, Int. J. Appl. Ceram. Technol. 8 (2011) 610–616, https://doi.org/10.1111/j.1744-7402.2009.02468.x.
[22] V. Piotter, W. Bauer, R. Knitter, M. Mueller, T. Mueller, K. Plewa, Powder injection moulding of metallic and ceramic micro parts, Microsyst. Technol. 17 (2011) 251–263, https://doi.org/10.1007/s00542-011-1274-2.
[23] V. Piotter, E. Honza, A. Klein, T. Mueller, K. Plewa, Powder injection moulding of multi-material devices, Powder Met. 58 (2015) 344–348, https://doi.org/10.1179/0032589915Z.000000000256.
[24] T. Moritz, A. Mannschatz, 2C ceramics moves into the industrial reality zone, Met. Powder Rep. 65 (2010) 22–25, https://doi.org/10.1016/S0026-0657(10)70071-0.
[25] J.L. Johnson, L.K. Tan, P. Suri, R.M. German, Design guidelines for processing bi-material components via powder-injection molding, JOM 55 (2003) 30–34, https://doi.org/10.1007/s11837-003-0172-1.
[26] V. Piotter, G. Finnah, B. Zeep, R. Ruprecht, J. Haußelt, Metal and ceramic micro components made by powder injection molding, Mater. Sci. Forum 534–536 (2007) 373–376, https://doi.org/10.4028/www.scientific.net/MSF.534-536.373.
[27] A. Milovanović, M. Milošević, G. Mladenović, B. Likozar, K. Čolić, N. Mitrović, Experimental dimensional accuracy analysis of reformer prototype model produced by FDM and SLA 3D printing technology, in: N. Mitrovic, M. Milosevic, G. Mladenovic (Eds.), Exp. Numer. Investig. Mater. Sci. Eng., Springer International Publishing, Cham, 2019, pp. 84–95.
[28] T. Uchiyama, W. Jiang, Molybdenum disilicide heating element and its production method, US 6,211,496 B1, 2001.